
Research Paper

The Role of Molecular Structure in the Crystal Polymorphism of Local Anesthetic Drugs: Crystal Polymorphism of Local Anesthetic Drugs, Part X

Andrea C. Schmidt

Received March 9, 2005; accepted August 22, 2005

Purpose. This report is the résumé of a comprehensive investigation on the solid-state properties and the crystal polymorphism of the structurally homogenous class of local anesthetic drugs. The goal is to explore the relationship between crystal polymorphism and molecular structural features.

Methods. A salt form (mostly the hydrochloride) as well as the free base of 24 local anesthetics has been characterized by means of thermomicroscopy, differential scanning calorimetry, pycnometry, Fourier transform infrared, Fourier transform Raman, and solid-state NMR spectroscopies, as well as X-ray diffraction methods (single crystal, powder).

Results. Based on the thermochemical data, the relative thermodynamic stabilities of the different crystal forms of each polymorphic system were evaluated and visualized as semiquantitative energy/temperature diagrams.

Conclusion. This study is the first step in recognizing relationships between the structure and the solid-state properties within this limited group of active substances with common structural elements. The results clearly show that there are certain relationships, but, to understand the phenomenological behavior in more detail on a molecular level, more structural information must be collected and analyzed by computational methods.

KEY WORDS: conformational polymorphism; local anesthetics; solid-state properties; spectroscopy; thermal analysis.

INTRODUCTION

Different solid forms that can be found on a pharmaceutical compound are polymorphs, solvates (pseudopolymorphs), desolvates, and amorphous solids. Polymorphs consist of the same chemical composition, but they show different arrangements of conformationally equivalent molecules or different conformers (conformational polymorphism) or both within the crystal lattice. More than 50% of drug molecules show polymorphism (1), and a great number of polymorphic pharmaceuticals are published (2,3).

Crystal solvates (pseudopolymorphs) are crystalline solid adducts between a compound and a solvent. The solvent can appear as a stoichiometric or nonstoichiometric related component of the lattice. If the included solvent is water, the solvate is named hydrate. Solvent adducts may easily crystallize because two molecules often can pack easier than single molecules, possibly caused by adduct symmetry, adduct-induced conformational changes, and the ability to form hydrogen bonds between the solvent and the pharmaceutical compound (4).

Desolvated solvates are crystals derived from the desolvation of a solvate keeping the structural characteristics of the solvate. Desolvated solvates often are less organized and

difficult to characterize. This type of solid form only can be received from the solvate, often is unstable, and shows a high affinity to the solvent, which was incorporated in the crystal lattice. Dehydrated hydrates often absorb water from the air to stabilize the crystal structure by filling the vacant positions with water molecules. The analytic results show them as unsolvated (anhydrous) materials, but in fact, they own the structure of the solvated crystal form from which they appeared (5).

Although amorphous solids (glasses) are commonly formed by molecules of large molecular size, like polymers and proteins, glasses of small-molecule organics are not uncommon. Pharmaceutical processes, like milling, solid dispersions, freeze-drying, and spray drying, are capable of producing amorphous solids, which are generally less stable physically and chemically, less dense, more soluble, faster dissolving/subliming, and more hygroscopic than their crystalline counterparts (6).

Because of the physical differences, the solid forms show different melting and sublimation temperature, heat capacity, conductivity, volume, density, crystal shape, color, refractive index, solubility, dissolution rate (7), stability, hygroscopicity, and sometimes bioavailability (8) or toxicity (9).

In spite of the indispensability of the solid-state characterization in the early development stage of a pharmaceutical compound, there exists no reliable model to predict crystal structures and polymorphism. Many scientists focus their research on the computational prediction of crystal structures

Department of Pharmaceutical Technology, University of Innsbruck, Innrain 52, 6020 Innsbruck, Austria.
To whom correspondence should be addressed. (e-mail: andrea.schmidt@uibk.ac.at)

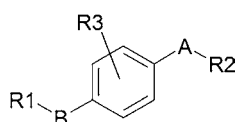


Fig. 1. General formula of local anesthetics.

and polymorphism (10–14), but none of these approaches can make the experimental polymorph screening unnecessary at this time.

For this study, the class of local anesthetic (LA) compounds was chosen because of its conformity of structural composition (Fig. 1) and its relatively high number of polymorphic representatives. The local anesthetics are separated into three groups, named after the type of molecular linking between hydrophilic and lipophilic moieties [the hydrophilic group is responsible for the receptor binding, whereas the lipophilic and the linking groups affect the duration of action

(15)]: ester type (LAE) with short duration of action, amide type (LAA) with medium or long duration of action, and a third group with different molecular structures, e.g., ketones or ethers. The molecular structures of the local anesthetics used for this study are listed in Table I.

There are several analytical methods to characterize a distinct crystal form of a compound during processing and different developmental stages. Information about the crystal structure of crystalline solids is provided by single crystal X-ray diffraction (16). Powder X-ray diffraction (PXRD) gives a fingerprint of a distinct crystal form and sometimes can be used for the determination of a crystal structure. For further characterization of polymorphic and pseudopolymorphic crystal forms, spectroscopic methods [infrared (IR), Raman, solid-state nuclear magnetic resonance (SSNMR), UV-vis, and fluorescence] can be applied. Thermal analytic methods are of special interest (17) for the determination of the thermodynamic relationship of the different polymorphs, in

Table I. Molecular Structures of the Local Anesthetics of This Study

| Group | A | B | R1 | R2 | R3 | Compound | |
|---------|------------------|---|----|----|----|----------------|-------------------|
| LAE | Benzocaine group | | | | | | Benzocaine |
| | | | | | | | Butambene |
| | | | | | | | Isobutambene |
| | Procaine group | | | | | | Procaine |
| | | | | | | | Chloroprocaine |
| | | | | | | | Hydroxyprocaine |
| | | | | | | | Dimethocaine |
| | | | | | | | Leucinocaine |
| | | | | | | | Butacaine |
| | | | | | | | Oxybuprocaine |
| | Tetracaine group | | | | | | Tetracaine |
| | | | | | | | Hydroxytetracaine |
| | | | | | | | Cornecaine |
| | POB | | | | | | Butoxycaine |
| | | | | | | | Proxymetacaine |
| | | | | | | Parethoxycaine | |
| | | | | | | Surfacaine | |
| Ether | | | | | | Pramocaine | |
| Ketones | | | | | | Dyclonine | |
| | | | | | | Propipocaine | |
| LAA | | | | | | Prilocaine | |
| | | | | | | Mepivacaine | |
| | | | | | | Bupivacaine | |
| | | | | | | Lidocaine | |
| | | | | | | Cinchocaine | |

LAA: Amide-type local anesthetics; LAE: ester-type local anesthetics; POB: *p*-oxy-benzoic group; PAB: *p*-aminobenzoic group.

particular, differential scanning calorimetry (DSC), thermogravimetric analysis (TGA), and hot stage microscopy (HSM).

In this study, the crystal forms of 49 local anesthetic active compounds were identified and characterized by HSM, DSC, TGA, IR, Raman spectroscopy, PXRD, and water sorption analysis and partially by SSNMR, pycnometry, and single crystal X-ray diffractometry (SCXRD). The relative thermodynamic and kinetic stabilities of the polymorphs were determined and evaluated in a semischematic energy/temperature diagram for each of the compounds.

MATERIALS AND METHODS

Materials

One to nine commercial samples of each compound from various companies were available for this study. All solvents used in this study were of “pro-analysis” quality.

Methods

Hot Stage Microscopy

The thermal behavior of the solid-state forms was observed using an Olympus BH-2 polarizing microscope (Olympus Optical Co., Ltd., Tokyo, Japan), equipped with a Kofler hot stage (Reichert, Vienna, Austria), and linked with a digital camera (Olympus DP50, Olympus Optical Co., Ltd.) using AnalySIS Image Processing software.

Differential Scanning Calorimetry

Differential scanning calorimetry thermograms were recorded with a DSC7 system (Perkin-Elmer, Norwalk, CT, USA) using the Pyris 2.0 software. Samples of approximately 2 mg (weights controlled to ± 0.0005 mg using a UM3 ultramicrobalance, Mettler, Greifensee, Switzerland) were weighed into aluminum pans (25 μl) with perforated covers. Dry nitrogen was used as a purge gas (purge, 20 ml min^{-1}), and the system was calibrated with caffeine (236.4°C) and indium 99.999% (156.6°C, 28.45 J g^{-1}). Heating rates of 5 K min^{-1} were routinely used.

Thermogravimetry

Thermogravimetric analysis was performed with a TGA7 system (Perkin-Elmer) using the Pyris 2.0 software. Samples of approximately 5 mg (weights controlled to ± 0.0005 mg using a UM3 ultramicrobalance, Mettler) were weighed into aluminum pans (15 μl). Two-position calibration of the temperature was performed with ferromagnetic Ni (ferromagnetic transition 163°C) with respect to the standard of Perkin-Elmer. Heating rates of 5 K min^{-1} were routinely used (except isothermic runs). Dry nitrogen was used as a purge gas (sample purge, 20 ml min^{-1} ; balance purge, 40 ml min^{-1}).

Infrared Spectroscopy

Fourier transform infrared (FTIR) spectra were acquired on a Bruker IFS 25 spectrometer (Bruker Analytische

Messtechnik GmbH, Karlsruhe, Germany). Spectra over a range of 4000–400 cm^{-1} with a resolution of 2 cm^{-1} (50 scans) were recorded using KBr pellets [approximately 2 mg sample compound per 300 mg KBr]. For temperature-controlled FTIR spectra, the samples were prepared on ZnSe disks using a heating device (Bruker) and the Bruker IR microscope I (Bruker Analytische Messtechnik GmbH), with 15 \times Cassegrain objectives (spectral range 4000–600 cm^{-1} , resolution 4 cm^{-1} , 100 interferograms per spectrum).

Raman Spectroscopy

Raman spectra were recorded with a Bruker RFS 100 Raman spectrometer (Bruker Analytische Messtechnik GmbH), equipped with a Nd:YAG laser (1064 nm) as excitation source and a liquid-nitrogen-cooled, high-sensitivity Ge detector. The spectra were recorded in aluminum sample holders at a laser power of 300 mW (64 scans per spectrum).

Solid-state NMR

High-resolution ^{13}C spectra of the solid-state forms (or mixtures of forms) were obtained at 75.43 MHz using a Varian Inova spectrometer. Magic-angle spinning at rates of ca. 4.5 kHz was employed, with a Doty probe accepting 7-mm-O.D. rotors. The dipolar dephasing (“nonquaternary suppression”) pulse sequence was used to select spectra containing signals from quaternary and methyl carbons only to assist in the assignment processes.

The ^{13}C chemical shifts were referenced by replacement to the signals for solid adamantane (high-frequency peak set to $\delta_{\text{C}} = 38.4$ ppm) but are quoted with respect to the standard tetramethylsilane.

Powder X-ray Diffractometry

The X-ray diffraction patterns were obtained using a Siemens D-5000 diffractometer (Siemens AG, Karlsruhe, Germany) equipped with a theta/theta goniometer, a Goebel mirror (Bruker AXS, Karlsruhe, D), a 0.15° soller slit collimator, and a scintillation counter. The patterns were recorded by $\text{CuK}\alpha$ -radiation, $\lambda = 1.54056$ Å, at a tube voltage of 40 kV and a tube current of 35 mA, applying a scan rate of 0.005° $2\theta \text{ s}^{-1}$ in the angular range of 2–40° in 2θ . Temperature- and moisture-controlled experiments were performed with a low-temperature camera TTK (Anton Paar KG, Graz, Austria) and a SYCOS-H humidity control system (Asynco, Karlsruhe, Germany).

Single Crystal X-ray Diffractometry

X-ray diffraction data of suitable single crystals were recorded with Smart CCD platform 3-circle diffractometer (Bruker AXS) using graphite monochromatized $\text{MoK}\alpha$ -radiation, $\lambda = 0.71073$ Å, from a sealed tube operated at 50 kV/40 mA. A Kryoflex cooling unit (Bruker AXS) was applied where appropriate. Complete spheres of the reciprocal space up to $\theta_{\text{max}} = 25$ –28° were scanned by each four

swings of 600 ω -scan frames ($\Delta\omega = 0.3^\circ$) at $\varphi = 0, 90, 180,$ and 270° . The frame data were integrated with the program SAINT, corrected for absorption (multiscan method) and $\lambda/2$ with the program SADABS, and were then analyzed with the program XPREP. Initial structure solutions were obtained with direct methods using the program SHELXS97. Least-squares refinements with anisotropic displacement parameters for nonhydrogen atoms were based on F^2 and the program SHELXL97.

Water Vapor Sorption Analysis

The moisture sorption isotherms were acquired using a SPS-11 moisture sorption analyzer (MD Messtechnik, Ulm, Germany). The measurement cycles were started at 0% relative humidity (RH) and were increased in 10% steps up to 90% RH and then back to 0% RH. The equilibrium condition for each step was set to a weight constancy of $\pm 0.007\%$ over 40 min. The temperature was $25 \pm 0.1^\circ\text{C}$.

Pycnometry

Volume and density determination were carried out on an Ultrapycnometer 1000 (Quantachrome Corp., Syosset, NY, USA) with helium purge, sample weights of 2–3 g, and calibration volume of 1.0725 ml.

Freeze-drying

Solutions were prepared at concentrations of 5 and 10% w/w in aqueous solutions. The frozen aqueous solutions were transferred to a Lyolab B, LSL freeze-dryer (Secroid Lyophilisator Inula, Vienna, Austria), equipped with vacuum pump 2400 A (Alcatel Cit, Annecy Cedex, France). The samples were dried at -60°C for 50 h (0.05-mbar chamber pressure).

RESULTS AND DISCUSSION

Classification by Molecular Structure

In this study, polymorph screenings on 49 local anesthetic compounds (55% free bases and 45% salts) were systematically examined. Most of the salts are hydrochlorides (88%), with the advantage of being slightly soluble in water, two are sulfates, and one is a mesylate, which was found not to influence the occurrence of polymorphism. For statistical evaluation, the compounds were separated into free bases and (hydrochloride) salts as shown in Fig. 2. In the next evaluation step, the compounds were separated into groups with regards to structural aspects (Table I). The benzocaine (BZC) group consists of the three bases benzocaine, butambene, and isobutambene, which commonly are used as bases in pharmaceutical topical preparations. The procaine group is characterized by the unsubstituted *p*-aminobenzoic (PAB) group with different moieties in the hydrophilic part of the molecule (Fig. 1, A-R2), whereas the tetracaine group shows substituted PAB structure. The *p*-oxybenzoic (POB) esters show structural similarities to the PAB, with the amino group replaced by oxygen. Ether and ketones exhibit different types of linking between the lipophilic (Fig. 1, Ph-B-R1) and the hydrophilic parts of the molecule. LAA strongly differ from LAE with regards to the lipophilic and the hydrophilic parts of the molecule.

Occurrence of Polymorphism and Pseudopolymorphism

Whereas only every fifth base was found to be polymorphic with a maximum of two polymorphs, two thirds of the hydrochloride salts are able to crystallize in more than one crystal form (with two to four polymorphs). Figure 3 shows the distribution of polymorphism and pseudopolymorphism with regards to the structural groups. The salts of the tetracaine group, ethers, ketones, and bases of the

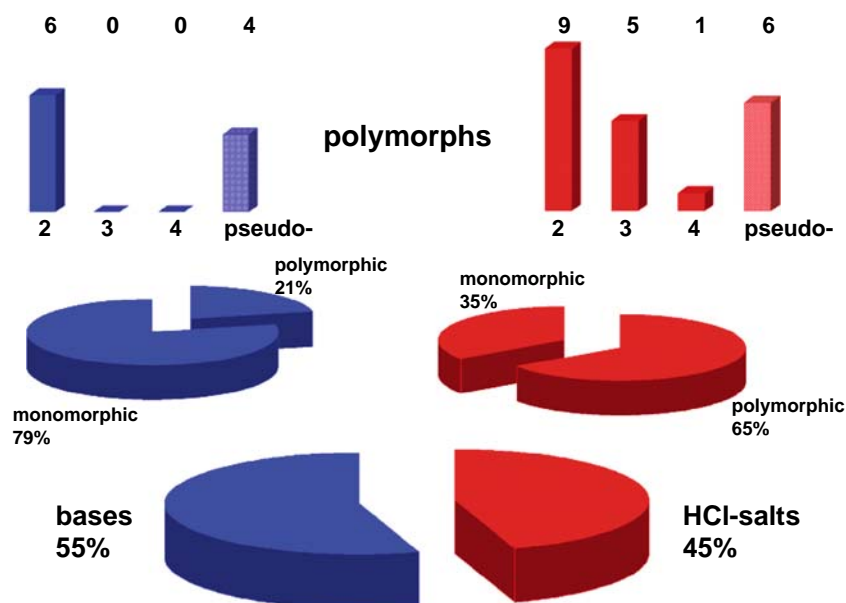


Fig. 2. Occurrence of polymorphism and pseudopolymorphism within the local anesthetics investigated in this study.

benzocaine group are polymorphic compounds, whereas the POB group in both categories (salts and bases) show less polymorphism; however, the LAA group showed more cases of pseudopolymorphism as compared to LAE and ethers/ketones.

Preparation and Characterization of Different Solid Phases

The crystal forms are named according to the notation of Kofler and Kofler (18) using roman numerals in the order of the melting points (i.e., the form with the highest melting point is called mod. I). A modification, which is thermodynamically stable at 20°C, is marked with a superscript zero. The polymorphs and their melting points found in this study are listed in Table II.

New crystal phases of the compounds of this study were found by slow or fast crystallization from the melt at different temperatures or solid–solid transition (HSM, DSC), from slow or fast crystallization from different solvents, and/or from freeze-drying. Fast crystallization mostly induced the less stable polymorph (19), e.g., tetracaine hydrochloride (TCHC) (20) and BZC (21). Freeze-drying mostly resulted in the stable crystal form, and also a new polymorph [salicaine hydrochloride (SLCHC)] (22), a hydrate [hydroxyprocaine hydrochloride (HPCHC)] (23), and an amorphous solid [prilocaine hydrochloride (PRCHC)] (24) were received from freeze-drying. The solvents routinely used for crystallization experiments were ethanol, ethanol 70%, methanol, 1-propanol, 2-propanol, 1-butanol, 1-pentanol, acetone, aceto-

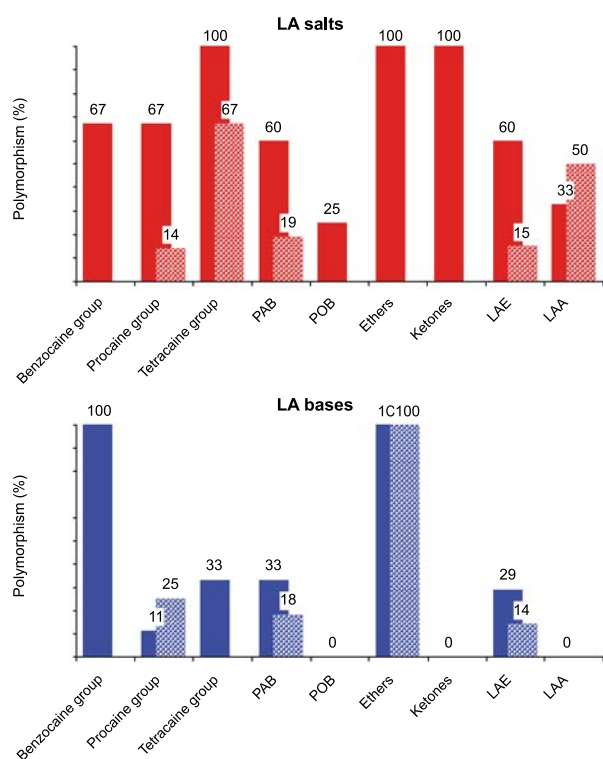


Fig. 3. Distribution of polymorphism and pseudopolymorphism on the structural groups of local anesthetics. Hatched columns mark formation of hydrates.

Table II. Melting Points of Local Anesthetics Determined in this Study by Differential Scanning Calorimetry Using Heating Rates of 5 K min⁻¹

| Compound | Abbreviation | Melting point (°C) | | | | |
|-----------------------|--------------|--------------------|-----|-----|-----|---------|
| | | IV | III | II | I | H |
| Benzocaine | BZC | | | 90 | 90 | |
| Benzocaine HCl | | | | | 195 | |
| Bupivacaine | | | | | 107 | |
| Bupivacaine HCl (RS) | BPCHC | | | | 257 | 112 |
| S-Bupivacaine HCl | | | | 144 | 255 | |
| R-Bupivacaine HCl | R-BPCHC | | | 144 | 255 | |
| Butacaine | | | | | 37 | >25 |
| Butacaine HCl | | | 115 | 131 | 151 | |
| Butacaine sulfate | | | | | 102 | |
| Butambene | BTN | | | 56 | 58 | |
| Butambene HCl | | | | | 187 | |
| Butoxycaine | | | | | <25 | |
| Butoxycaine HCl | | | 104 | nd | 148 | |
| Chloroprocaine | | | | | <25 | |
| Chloroprocaine HCl | 2-CPCHC | | | nd | 172 | |
| Cinchocaine | | | | | 64 | |
| Cinchocaine HCl | CCCHC | | | | 90 | |
| Cornecaine | | | | | 78 | |
| Cornecaine HCl | CCHC | | | 133 | 136 | |
| Dimethocaine | | | | | 53 | |
| Dimethocaine HCl | | | | | 199 | |
| Dyclonine | | | | | <25 | |
| Dyclonine HCl | DCNHC | | | 174 | 175 | |
| Hydroxyprocaine | | | | | <25 | |
| Hydroxyprocaine HCl | HPCHC | | | 154 | 160 | 144 |
| Isobutambene | BTI | | | 48 | 55 | |
| Leucinocaine | | | | 32 | 39 | |
| Leucinocaine mesylate | LCCM | | | 158 | 171 | |
| Lidocaine | LDC | | | | 68 | |
| Lidocaine HCl | LDCHC | | | | 129 | 77 |
| Mepivacaine | | | | | 150 | |
| Mepivacaine HCl (RS) | MPCHC | | | | 265 | |
| Oxybuprocaine | | | | | <25 | |
| Oxybuprocaine HCl | OBPHC | | 146 | 149 | 160 | |
| Pramocaine | | | | 11 | 24 | >25 |
| Pramocaine HCl | PMCHC | | 139 | 154 | 172 | |
| Prilocaine | | | | | 37 | |
| Prilocaine HCl | PRCHC | | | 165 | 169 | |
| Procaine | PC | | | | 51 | >25 |
| Procaine HCl | PCHC | | | | 156 | |
| Proparacaine | | | | | <25 | |
| Proparacaine HCl | | | | | 183 | |
| Propipocaine | | | | | <25 | |
| Propipocaine HCl | PPCHC | | | 165 | 166 | |
| Salicaine | SLC | | | | 46 | |
| Salicaine HCl | SLCHC | | 148 | 151 | 157 | 143 |
| Surfacaine | | | | | <25 | |
| Surfacaine sulfate | | | | | 162 | |
| Tetracaine | | | | 37 | 42 | |
| Tetracaine HCl | TCHC | 136 | 139 | 142 | 147 | 88; 108 |

H: Hydrate; nd: not determined.

nitrile, methylene chloride, trichloromethylene, diethyl ether, ethyl acetate, *n*-hexane, cyclohexane, 1,4-dioxane, nitromethane, ethyl methyl ketone, dimethylformamide, and toluene. Nevertheless, solid–solid transitions, which were induced by moisture, could be observed by water vapor sorption studies (PRCHC and HPCHC). Sublimation of the compounds always

resulted in pure crystals melting together with the high-temperature form.

Thermal Analysis

Hot Stage Microscopy

All of the commercial products show highly birefringent crystals of the pure thermodynamically stable forms except TCHC, SLCHC, and HPCHC, which are partly contaminated with their hydrated form. On heating up to 60°C using a heating rate of 5 K min⁻¹, these crystals start to jump and to crack intensely, which are probably caused by dehydration. The loss of water does not cause significant change of polarized colors, whereas the former plane crystal shapes show a fine lamellation (Fig. 4A) after the thermal dehydration. Most of the compounds start to condense (25), and sublimates with different shapes precipitate on the slide (Fig. 4B–D). On heating, the rate of precipitation is incessantly increasing until the temperature reaches the melting point. The sublimates melt together with the high-temperature modification of the respective compound (at the same temperature). The melting points mostly coincide with the melting points given in the literature (26–29). None of the compounds melt under decomposition, but some compounds are thermally unstable at temperatures right above their melting point (SLCHC, HPCHC) and can only be kept in the liquid phase for a short time (<1 min). The thermodynamically stable crystal forms mostly crystallize shaped as spherulites from the melt (Fig. 4E), whereas the high-temperature forms crystallize in colored planes (Fig. 4F). All crystal phases can be received as pure forms except butoxycaïne hydrochloride from the POB group, which crystallizes as concomitant polymorphs (30) (Fig. 4G). In preparations with highly viscous silicone oil, the hydrated crystals are observed to loose water (Fig. 4H) between 40 and 80°C, which indicates less stable hydrates (see Moisture Sorption).

Differential Scanning Calorimetry

Most of the polymorphic compounds of this study (benzocaine group, POB, and ether and ketones groups) show solid–solid transitions between the polymorphs. All compounds of the tetracaine group and some of the procaine group show inhomogeneous melting, which means that another polymorph is crystallizing from the melt while one form is melting (Fig. 5). If the stable forms of TCHC, SLCHC, and HPCHC include some water, they melt inhomogeneously, but if these crystals were dried in an oven before at 100°C, they will melt without nucleation and crystallization of mod. I. In these cases, the nucleation of the high-temperature form is induced by moisture (see Moisture Sorption). These compounds additionally form hydrates by recrystallization from water or under moist air. The hydrates exhibit an endothermic melting peak in a sealed pan. In a pan with perforated cover, the included water leaks with increasing temperature, and only the endothermic melting peak of mod. I is registered. The enthalpy difference between the two polymorphic forms is about 10 kJ mol⁻¹, which is a high value compared to the other local anesthetics. The compounds of the benzocaine group have transition points at lower

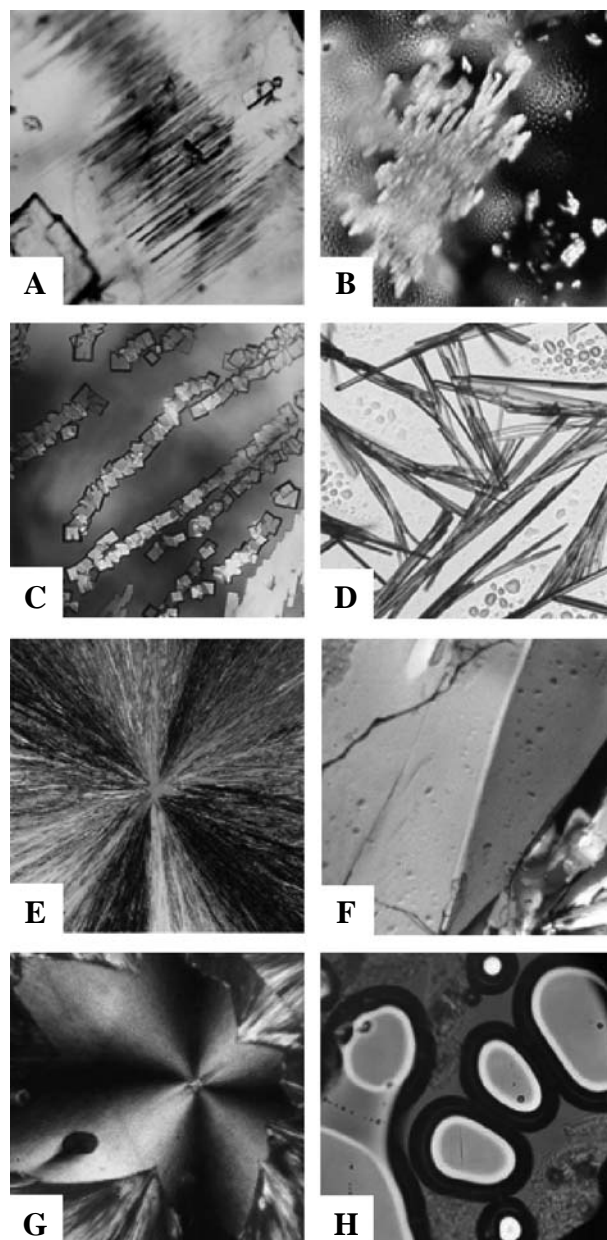


Fig. 4. Micrographs from hot stage microscopy. (A) Lamellation of tetracaine hydrochloride (TCHC) dehydrated crystal. (B–D) Sublimates of oxybuprocaine hydrochloride (OBPHC), benzocaine, and 2-chloroprocaine hydrochloride. (E) Spherulite of OBPHC mod. II. (F) Plates of TCHC mod. I. (G) Concomitant polymorphs of butoxycaïne hydrochloride. (H) Dehydration of TCHC hydrate in a silicone oil preparation.

temperatures, so the “high-temperature forms” are the thermodynamically stable forms at room temperature, i.e., the transition temperatures lie below room temperature. The compounds of all other LA groups have transition points at higher temperatures than room temperature. Some compounds [oxybuprocaine hydrochloride (OBPHC) (25) and pramocaine hydrochloride (PMCHC)] (31) show reversible solid–solid transitions to a low-temperature form (mod. III) when cooling the crystals as well as to a high-temperature form (mod. I) when heating the crystals.

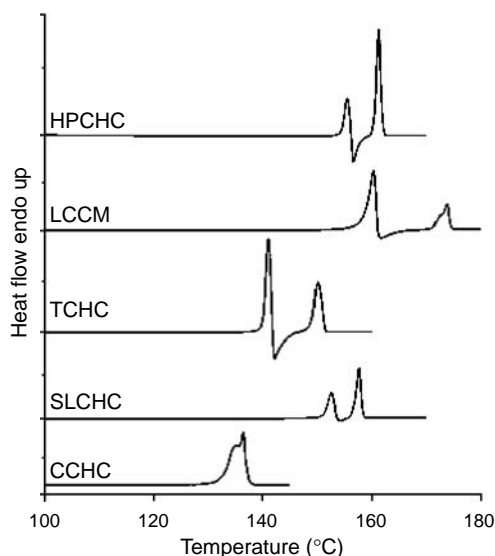


Fig. 5. Differential scanning calorimetry curves of the stable modifications of compounds of the procaine and tetracaine group. Heating rates, 5 K min⁻¹.

Thermogravimetric Analysis

From the LAE, only TCHC, SLCHC, and HPCHC form solvates (hydrates). Thermogravimetry of SLCHC and HPCHC shows a nearly continuous weight loss using a heating rate of 5 K min⁻¹ with a small bend in the curve progression, where water desorption has stopped and decomposition of the compound starts. The thermal stability of HPCHC compared to procaine hydrochloride (PCHC) and of SLCHC compared to TCHC (same molecular structures but without hydroxylic group) is strongly reduced by the hydroxylic moiety in the paraposition of the phenyl ring. The water content of these hydrates ranges from 1.9 to 2.7% (related to the weight of the hydrated form, 0.3–0.6 mol) at room conditions. Isothermic gravimetric investigations showed that the compounds loose water between 30 and 60°C, and the water can entirely be removed from the crystals, which shows that the water is loosely arranged in these crystals and easily can be removed by thermal means without thermal decomposition of the compounds. From the thermogravimetric curve progression, we conclude that TCHC, SLCHC, and HPCHC form nonstoichiometric hydrates (see Moisture Sorption). The solvates and hydrates of the LAA [lidocaine hydrochloride (LDCHC), bupivacaine hydrochloride (BPCHC), and PRCHC] are stoichiometric, and their stability to desolvation is evidently higher.

Spectroscopy

FTIR and Raman Spectroscopy

The IR and Raman spectra of the LA polymorphs show generally small (because of conformational polymorphism) but reproducible differences. The band shifts normally average to 3–6 cm⁻¹, and the most striking differences can be realized in the range of the C–H stretching vibrations of the alkyl chain (3000–2900 cm⁻¹, Raman), probably

caused by different arrangements of the methylene groups (asymmetric CH-stretching vibrations). Smaller differences were found in the range of νC=O (1700–1600 cm⁻¹, FTIR), the stretching vibrations of hydrogens of the NH₂ moiety and hydrogen bondings (3450–3220 cm⁻¹, FTIR), and the molecule vibrations (1500–1000 cm⁻¹, FTIR). The polymorphs can be easily differentiated by the lattice vibrations (200–50 cm⁻¹, Raman).

The highest infrared bonds (N–H or O–H stretching vibration, 3500–3300 cm⁻¹) in the infrared spectra of the stable forms of HPCHC, 2-chloroprocaine hydrochloride (2-CPCHC), TCHC, SLCHC, OBPHC, and leucocaine mesylate lie at higher wave numbers (Table III) than those of the respective unstable forms. This suggests higher entropy and less stability for the forms, which are related to the free-energy curves, the thermodynamically stable forms at room temperature. This is contradictory to the infrared rule (IRR) (32,33) and suggests that intermolecular hydrogen bonding to the N1 amino function is not the driving force in the molecular arrangements of these crystal forms. Burger and Ramberger showed that all exceptions of the IRR have at least one CO–NH group, which is not the case in the LAE molecules. But it is reasonable that the vinyl moiety, which separates the CO and the NH group in the LAE molecules (see Table I and Fig. 1, hydrophilic part of the molecules, A–R2), causes the same structural behavior (34). Thirty-one percent of our systematically examined LA do not fulfill the IRR, which is a relatively high number of IRR exceptions, whereas Burger and Ramberger expected 10% exceptions of the IRR.

NMR Spectroscopy

¹³C, ¹H, and ¹⁵N solid-state NMR spectra of the polymorphic compounds prove to be a very useful method to qualify molecular differences between the polymorphs and to determine the number of conformers in the asymmetric unit. ¹³C CP MAS NMR spectra of HPCHC mod. II° and hydrated mod. I (Fig. 6) clearly show two conformers in the asymmetric unit of the hydrated mod. I indicated by doublets of peaks. The stable mod. II° consists of one conformer, which

Table III. Infrared Frequencies (νN–H or νO–H vibrations) Indicating Intermolecular Hydrogen Bondings of Thermodynamically Stable and Unstable Forms of Local Anesthetics Violating the Infrared Rule

| Compound | Infrared frequencies | | Trs |
|----------|----------------------|---------------|-----|
| | Stable form | Unstable form | |
| 2-CPCHC | 3433 (I°) | 3413 (II) | M |
| HPCHC | 3403 (II°) | 3384 (I) | E |
| LCCM | 3384 (II°) | 3380 (I) | E |
| OBPHC | 3469 (II°) | 3464 (I) | E |
| SLCHC | 3380 (II°) | 3302 (III) | M |
| SLCHC | 3302 (III) | 3266 (I) | E |
| SLCHC | 3380 (II°) | 3266 (I) | E |
| TCHC | 3377 (IV) | 3367 (I) | E |
| TCHC | 3380 (III°) | 3377 (IV) | M |
| TCHC | 3380 (III°) | 3367 (I) | E |

Trs: Solid–solid transition; E: enantiotropic; M: monotropic; ° : thermodynamically stable form at 20°C.

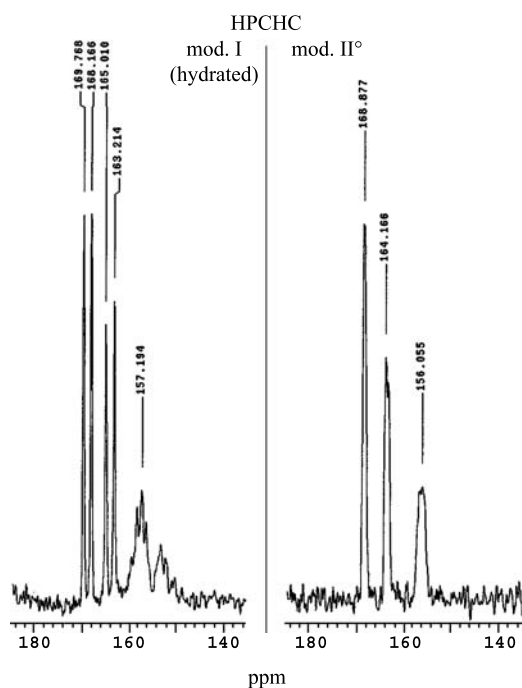


Fig. 6. ^{13}C solid-state nuclear magnetic resonance spectra of hydroxyprocaine hydrochloride (HPCHC) mod. I (hydrated) and mod. II $^{\circ}$ (both at ambient temperature) demonstrating the doublets of peaks (left) caused by the two molecules in the asymmetric unit of mod. I while mod. II $^{\circ}$ has only one.

is consistent with the crystallographic results. ^1H NMR (not shown) provides information about the strength of (intermolecular) hydrogen bondings. All of the compounds show relatively weak hydrogen bondings [a chemical deviation of 11.2 ppm (SLCHC mod. II $^{\circ}$) is the maximum value, which complies with the comparison of N–H and O–H stretching vibrations (infrared spectra) and the poor applicability of the IRR].

X-ray Diffractometry

Powder X-ray Diffractometry

The powder diffractograms best allow a clear and fast identification of the LA crystal forms because the conformational polymorphs differ a lot in their powder patterns. Most of the time, a record of the first small angles ($2\text{--}8^{\circ} 2\theta$) sufficiently identifies a distinct crystal form, which makes PXRD the method of first choice for fast differentiation between the crystal forms within a distinct LA polymorphic system. The patterns of TCHC, SLCHC, and HPCHC mods. I nearly show identical patterns to the respective hydrated forms (Fig. 7), so these crystal phases may be classified as isomorphous desolvates according to Stephenson *et al.* (35).

Single crystal X-ray diffractometry

During this study, single crystals of TCHC mod. IV, OBPHC mod. III, II $^{\circ}$, I, PRCHC dioxane solvate, SLCHC mod. II $^{\circ}$, hydrated mod. I, and SLC hydrate suitable for SCXRD could be produced, and the crystal structures were determined. The crystal structures of local anesthetics, which

were known before this study [BZC (36,37), procaine (PC) (38), PCHC (39,40), dyclonine hydrochloride (DCNHC) (41), LDCHC hydrate (42), BPCHC (43), BPCHC ethanolate, R-BPCHC (44), and mepivacaine hydrochloride (MPCHC) (45)], gave no indication on conformational polymorphism (Table IV) because they all show just one conformation of the molecule [except the monomeric LAA compounds lidocaine (LDC) (46) and cinchocaine hydrochloride hydrate (CCCHC) (47,48), which consist of two conformers in the asymmetric unit]. The polymorphic crystal structures of this study confirm that the crystal polymorphism of these compounds is caused by the conformational flexibility of the molecules (see Structural Aspects).

Pycnometry

Seventy-five percent of the examined polymorphic systems violate the density rule (DR) (32,33), which means that the crystal form with the higher density is not the more stable form. Any characteristic coherence between the molecular structure and the applicability of the density rule could not be found in this class of compounds.

Moisture Sorption

Moisture sorption was ascertained to be a useful tool to differentiate and identify the forms or rank polymorphic forms by their relative thermodynamic stability (with regard to surface area and crystal transformations). Representative sorption/desorption isotherms of LA crystal forms at 25°C are shown in Fig. 8. Mod. II $^{\circ}$, the thermodynamically and kinetically most stable form of SLCHC, adsorbs the smallest amount of water. A mixture of mod. II $^{\circ}$ and I, as present in one of the commercial samples, sorbs an amount of water being commensurate with the pure forms. At relative

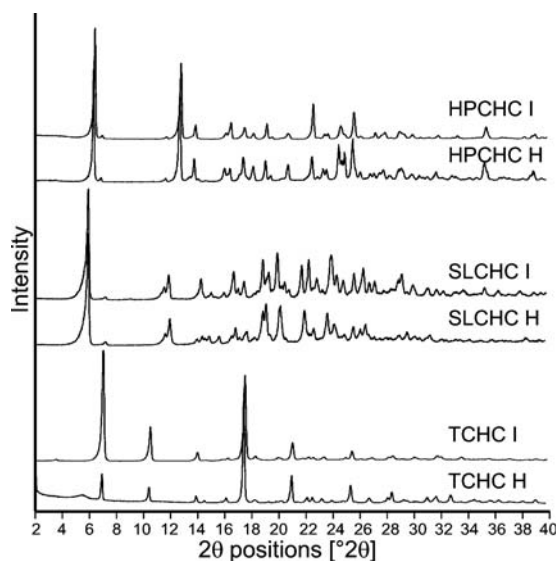


Fig. 7. Powder X-ray diffraction patterns of HPCHC, salicaine hydrochloride (SLCHC), and TCHC hydrates (H) and desolvated hydrates (I). Patterns of mod. I were recorded after recrystallization from the melt at 140°C under dry N_2 atmosphere. The differences in the peak intensities are attributed to preferred orientation. Recrystallization from the melt and from the dehydration of the hydrate results in the same pattern.

Table IV. Space Groups and Number of Conformers in the Asymmetric Units of Local Anesthetics

| Compound | Mod. | Space group | Conformers |
|--------------------|------------|---|------------|
| BPCHC | | P2 ₁ /n | 1 |
| BPCHC | Ethanolate | P2 ₁ | 1 |
| R-BPCHC | | P2 ₁ | 1 |
| BZN | | P2 ₁ 2 ₁ 2 ₁ | 1 |
| CCCHC | Hydrate | P2 ₁ /c | 2 |
| DCNHC | | P2 ₁ /a | 1 |
| LDC | | P2 ₁ /c | 2 |
| LDCHC | Hydrate | P2 ₁ /c | 1 |
| MPCHC | | P2 ₁ 2 ₁ 2 ₁ | 1 |
| OBPHC ^a | III | P2 ₁ /a | 2 |
| OBPHC ^a | II° | P2 ₁ /n | 2 |
| OBPHC ^a | I | C2/c | 1 |
| PC | | P2 ₁ /a | 1 |
| PCHC | | Pcab | 1 |
| PRCHC ^b | Dioxanate | P ⁻ 1 | 1 |
| SLC ^a | Hydrate | P ⁻ 1 | 2 |
| SLCHC ^a | II° | P2 ₁ /n | 1 |
| SLCHC ^a | I hydrated | P ⁻ 1 | 2 |
| TCHC ^a | IV | P ⁻ 1 | 1 |

^a Crystal structure solved in this study.

^b Jetti, personal communication.

humidities between 10 and 90% RH, a content of the hydrated form of 42–45% can be calculated for this commercial product from the sorption isotherms. In this case, the determination of the water content can be used as a fast and reliable method to quantify the degree of the mod. I impurity.

In the case of HPCHC, the stable mod. II° shows a significantly higher water uptake between 50 and 60% RH. At relative humidities above 60% RH, it sorbs nearly the same amount of water as the hydrate. The desorption curve of the former mod. II° proceeds according to the desorption curve of the hydrate. This clearly shows that above 50% RH, the increasing water vapor pressure induces a phase transition to the unstable mod. I, which is accompanied by a significantly high step in the sorption isotherm. The crystal system does not retransform to mod. II° on subsequent lowering of the relative humidity. This irreversible transformation was proved by moisture-controlled PXRD experiments. The hydrates of both compounds are characterized as non-stoichiometric hydrates being isomorphous with mod. I.

Polymorphs

A very useful tool for the comparison and evaluation of the polymorphic compounds is the semischematic energy/temperature diagram (49), which displays the thermodynamic relationship of the polymorphs of one system. Figure 9 shows a scheme of the possible transition pathways between all solid-state forms including the hydrates of TCHC along with the semischematic energy/temperature diagram of TCHC (four polymorphs). The energy/temperature diagram is based on the thermal analytical results and shows the relative thermodynamic stabilities of the polymorphs. Mod. III° is the most stable form between –273°C and its temperature of transformation to mod. I (T_{III-I}). Mod. I has the lowest stability at temperatures below the transition temperature

T_{IV-I} and the highest stability at temperatures above T_{III-I} (semischematically).

The isostructural compounds of the ketone group (DCNHC and PPCHC) (50) show analogy in their thermal analytical behavior, vibrational and NMR spectra, powder X-ray diffraction patterns, and even in their polymorphic behavior.

Polymorphs derived from solid–solid transitions were found to be kinetically less stable (31) than polymorphs crystallized from the melt or from a solvent.

Sixty-seven percent of the solid–solid transitions between the LA polymorphs are reversible, which is called enantiotropic. Thirty-three percent of the solid–solid transitions are monotropic, i.e., the higher melting phase is ener-

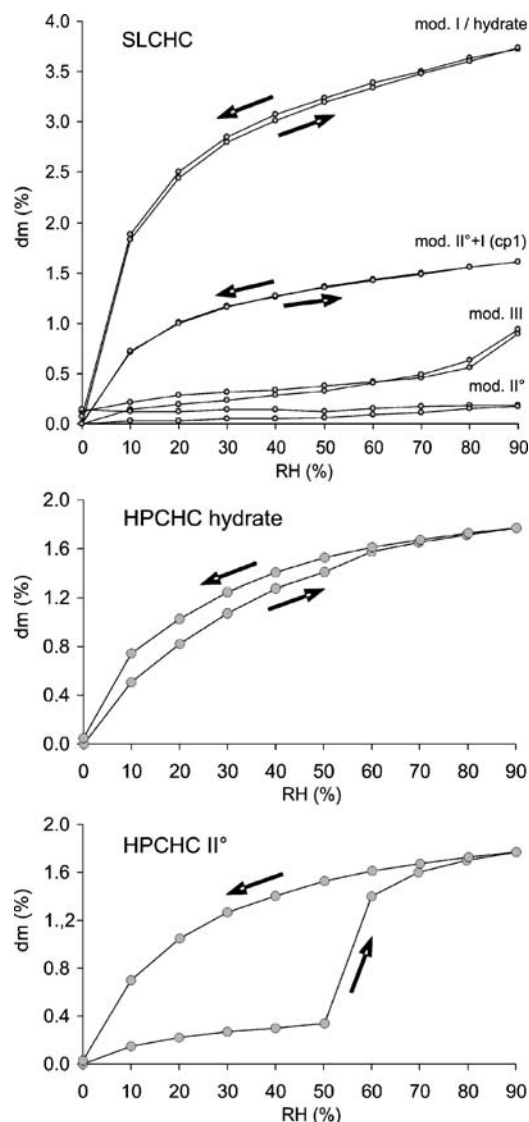


Fig. 8. Moisture sorption isotherms of SLCHC and HPCHC crystal forms at 25°C. The thermodynamically most stable form (mod. II°) sorbs the lowest amount of water, whereas the least stable (mod. I°) sorbs the most. HPCHC II° between 50 and 60% relative humidity (RH) shows a significantly higher water uptake. The desorption curve of the former mod. II° proceeds according to the desorption curve of the hydrate. The mass change is corrected for the minimum mass value at 0% RH. The measurement cycle started and ended at 0% RH.

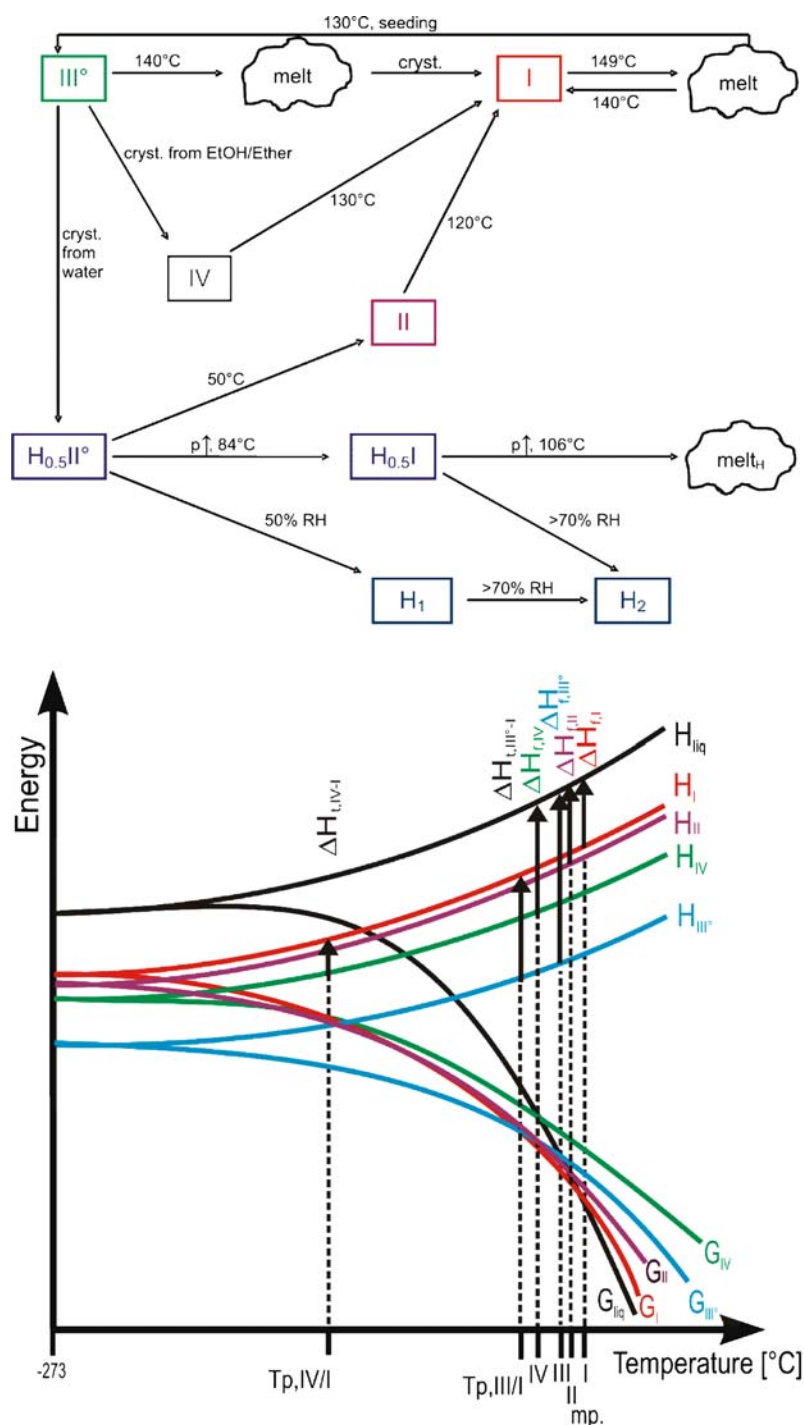


Fig. 9. Flow chart of TCHC crystal forms with transformation temperatures under ambient pressure conditions (above) and semischematic energy/temperature diagram of the polymorphs (bottom).

getically not able to transform to the lower melting phase. In these cases, the highest melting crystal form is the thermodynamically stable form in the entire temperature range below the melting point. The most number of monotropically related polymorphs was found in the group of POB. Other monotropic transitions appear in the procaine, tetracaine, and ether groups, where, respectively, the lowest melting polymorph (TCHC, SLCHC, OBPHC, PMCHC) is monotro-

pically related to the next polymorph, but both polymorphs are enantiotropically related to the highest melting polymorph. The polymorphs of the benzocaine and ketone group consistently are enantiotropically related. Any distinct coherence between the molecular structure and the reversibility of the transition between polymorphs could not be ascertained.

All of the compounds fulfill the heat of transition rule (32,33) or the heat of fusion rule, whereas a great number of

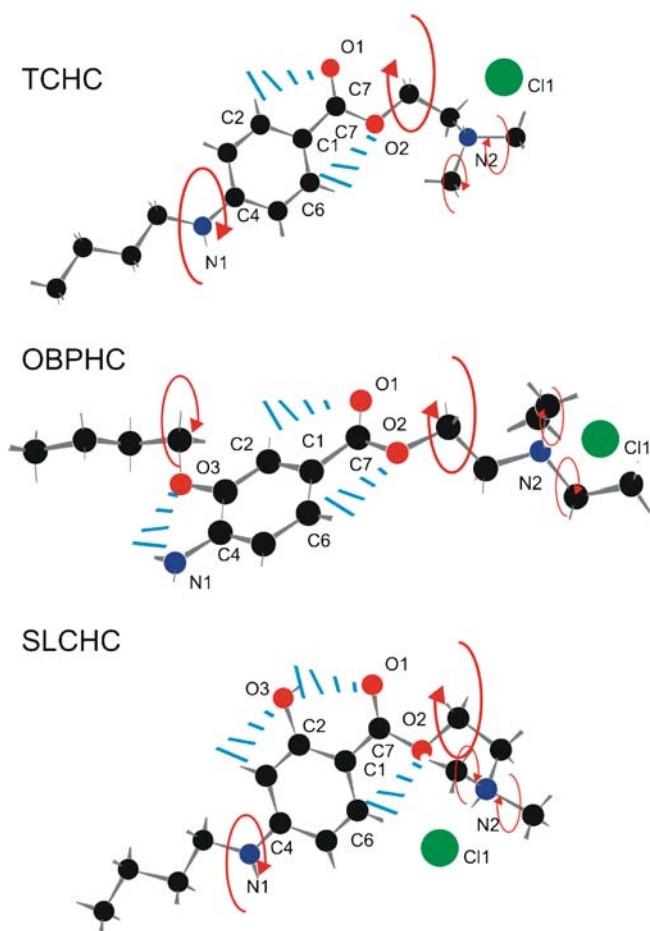


Fig. 10. Rotational flexibility of LAE molecules. The flexibility of the side chains of the OBPHC and SLCHC molecules (each three polymorphs) is reduced by different substituents of the planar phenyl ring compared to the TCHC molecule (four polymorphs). The crystal structures of SLCHC (Schmidt and Mereiter, unpublished data), OBPHC, and TCHC (unpublished data) were solved by SCXRD in this study.

exceptions of the DR (75%) and the IRR (59%) clearly discharge both rules from applicability in this class of compounds.

The rate of moisture sorption reliably indicates the thermodynamic ranking of the LA polymorphs. In all of the examined representatives, the thermodynamically less stable forms absorb higher amounts of water vapor than the more stable forms, even on compounds that show a very low affinity to water or do not tend to form hydrates. Moreover, the different moisture sorption rates of the polymorphs are independent of the factors whether a transition is enantiotropic or monotropic or whether the differences of melting enthalpies or the transition enthalpies are large or small. This conclusion is a first insight into the coherence between the stability of a crystal form and its water vapor sorption and should be further examined with respect to crystal size and surface area characteristics.

Solvates and Hydrates

Our systematic investigations on the solid-state properties of numerous local anesthetic drugs showed that in

contrast to LAA [e.g., PRCHC (51), LDCHC, and BPCHC], the LAE tend to form polymorphic crystal forms but less hydrates and solvates. Formation of hydrates was observed with both the free bases and the hydrochlorides. The multiple occurrence of solvated forms within the LAA was likely a result of the ability to form intermolecular hydrogen bonds with the N1 amide group (replaced by the ester group in the LAE). Just three compounds of the commonly known LAE with closely related structural features were also able to form hydrates: TCHC, SLCHC, and HPCHC. Freeze-drying of aqueous solutions of these compounds (10% w/w) led to fine powders of the hydrates.

Desolvated solvates

Desolvation of a solvate can lead to the solvent-free stable crystal form (BPCHC) (52), to another polymorph (PRCHC), to an isomorphic desolvate (TCHC, SLCHC, and HPCHC) (53), or to an amorphous solid (LDCHC) (54). All types of desolvated solvates were found within the LA, but the number is too small to draw a reliable conclusion on the structure–property relationship.

Amorphous Solids

Amorphous solids (glasses), which can be derived from a solution (e.g., evaporating solvent), from fast annealing of the melt, or by desolvation of a solvate, were only found with a few local anesthetics from the amide type (LAA): PRCHC, MPCHC, and LDCHC (53). These compounds form amorphous solids by lyophilization of aqueous solutions (10% w/w). Stable crystal forms occur on heating these glasses above 60°C (proved by PXRD). No relationship between molecular structure and formation of amorphous solids was found in this study.

Structural Aspects

The LAE molecules like TCHC show a high flexibility caused by the alkyl side chains in paraposition of the planar phenyl ring (Fig. 10). The rotational flexibility of the side chains additionally is increased by the N2 alkyl chains on the hydrophilic side of the molecule. A substituent in the meta-position of the phenyl ring like in the OBPHC molecule reduces the flexibility by an intramolecular hydrogen bond (N1–H...O3) and intramolecular interactions of the phenyl hydrogens (C2–H, C6–H) with the oxygen atoms O1 and O2. Thus, the atoms O1, N1, C7, O2, and O3 form a rigid plane motif with the phenyl ring in all three modifications of OBPHC. This planar structure unit allows a 180° rotation around the C1–C7 bond, maintaining the same interactions as mentioned above. If there is a substituent of the phenyl ring in the orthoposition (SLCHC, HPCHC, and 2-CPCHC) of the benzoic acid function, an additional intramolecular hydrogen bond (O3–H...O1) reduces the conformational flexibility and also the number of polymorphs.

The up-to-now structurally known LAE compounds (34–46) crystallize in monoclinic (64%), triclinic (21%), or orthorhombic (15%) space groups, but the organization or molecular packing in the crystals shows pronounced simi-

larities. Moreover, the protonated drug molecules in all cases (LAE and LAA) are linked by hydrogen bonds via the chloride anions forming parallel-orientated, infinite hydrogen-bonded chains. All triclinic crystal forms consist of two molecules in the asymmetric unit; all orthorhombic crystal forms show just one.

Whereas the molecules of the hydrochlorides (e.g., SLCHC) are arranged in chains connected by the moderately strong hydrogen bondings between N1–H and the chlorine atom (Cl1) to the N2–H of the neighbored molecule, the molecules of the free bases (e.g., SLC) are connected by weak hydrogen bondings between H–N1–H and the O1 of two neighboring molecules.

A missing flexible butyl side chain in molecules like HPCHC compared to SLCHC (also PCHC compared to TCHC) reduces the number of possible conformations, which is relevant for the formation of different (conformational) polymorphs like in many representatives of the LAE. Because of the missing butyl side chain, the HPCHC molecule forms less polymorphs, but the formation of a hydrate is not affected by the reduction of the flexibility of the molecule.

CONCLUSIONS

Crystal polymorphism: Local anesthetics of PAB show classic conformational polymorphism. The number of polymorphs increases with the increasing length of the alkyl chain in the para-position of the acid functional group. The *p*-oxy-substituted compounds (POB) form substantially less polymorphs, which is likely to be a result of a reduced conformational flexibility (stronger hydrogen-bonding effects). The water-soluble salts (mostly hydrochlorides) of the LA show more cases of polymorphism than the free bases, which are often liquid at 20°C. The hydrochloride salts form between two and four polymorphs on average.

Stability: The thermodynamic transition temperatures of the enantiotropically related modifications lie between 90 and 120°C with transition enthalpies of 3–4 kJ mol⁻¹. Only those PAB that form hydrates show unusually high enthalpies of transition (~17 kJ mol⁻¹). The compounds with a hydroxyl substituent in the C3 or C4 position of the phenyl ring are thermally labile. These compounds frequently show polymorphism and additionally nonstoichiometric hydrates, i.e., isomorphic desolvates. Benzocaine-like bases form enantiotropically related pairs of polymorphs with transition points at low temperatures. The ketones also crystallize in two enantiotropically related modifications and show similar melting properties to the ethers, which also can crystallize in a low-temperature form. The rate of moisture sorption reliably indicates the thermodynamic ranking of the LA polymorphs, which is a first insight into the coherence between the stability of a crystal form and its water vapor sorption, but should be further examined with respect to crystal size and surface area characteristics.

Molecular structure: The substitution of the C1 acid function does not influence the number of existing polymorphs. However, the substitution of the amino group in C4 position has a significant impact on the formation of different crystal forms. Formation of hydrates and solvates is a result of molecular level mechanisms (hydrogen bonding) different to the

mechanisms of polymorphism (conformational flexibility). In spite of different space groups, the organization or molecular packing in the crystals of all groups follows the same scheme (chains linked by hydrogen bonds). This study is the first step in recognizing relationships between the structure and the solid-state properties within this limited group of active substances with common structural elements. The results clearly show that there are certain relationships, but, to understand the phenomenological behavior in more detail on a molecular level, more structural information must be collected and analyzed by computational methods.

ACKNOWLEDGMENTS

The author thanks the European Science Foundation and the MORPH network for financial support. Many thanks are also due to Phuong Ghi, Andrew King, and Robin K. Harris for solid-state NMR measurements, to Gerhard Puerstinger for solution-state NMR measurements, to Thomas Brehmer, Kurt Mereiter, Ram Jetli, and Roland Boese for single-crystal XRD experiments and crystal structure solutions, to Elisabeth Gstrein for technical assistance, and to the following colleagues who have collaborated on the projects: Isabella Schwarz on the hydrates of tetracaine, hydroxytetracaine, and hydroxyprocaine, Nadja Senfter on pramocaine hydrochloride, and Verena Niederwanger on the local anesthetics of the amide type.

REFERENCES

1. J. O. Henck, U. J. Griesser, and A. Burger. Polymorphie von Arzneistoffen—Eine wirtschaftliche Herausforderung. *Pharm. Ind.* **59**:165–169 (1997).
2. L. Borcka and J. Halebljan. Crystal polymorphism of pharmaceuticals. *Acta Pharm. Jugosl.* **40**:71–94 (1990).
3. D. Giron. Investigations of polymorphism and pseudo-polymorphism in pharmaceuticals by combined thermoanalytical techniques. *J. Therm. Anal. Calorim.* **64**:37–60 (2001).
4. R. S. Vippagunta, H. G. Brittain, and D. J. W. Grant. Crystalline solids. *Adv. Drug Deliv. Rev.* **48**:3–26 (2001).
5. S. Byrn, R. Pfeiffer, M. Ganey, C. Hoberg, and G. Poochikian. Pharmaceutical solids: a strategic approach to regulatory considerations. *Pharm. Res.* **12**:945–954 (1995).
6. L. Yu, S. M. Reutzel, and G. A. Stephenson. Physical characterization of polymorphic drugs: an integrated characterization strategy. *Pharm. Sci. Technol. Today* **1**:118–127 (1998).
7. A. Panagopoulou-Kaplani and S. Malamataris. Preparation and characterisation of a new insoluble polymorphic form of glibenclamide. *Int. J. Pharm.* **195**:239–246 (2000).
8. A. J. Aguiar, J. Krc, A. W. Kinkel, and J. C. Samyn. Effect of polymorphism on the absorption of chloramphenicol from chloramphenicol palmitate. *J. Pharm. Sci.* **56**:847–853 (1967).
9. S. R. Chemburkar, J. Bauer, K. Deming, H. Spiwek, K. Patel, J. Morris, R. Henry, S. Spanton, W. Dziki, W. Porter, J. Quick, P. Bauer, J. Donaubaer, B. A. Narayanan, M. Soldani, D. Riley, and K. McFarland. Dealing with the impact of ritonavir polymorphs on the late stages of bulk drug process development. *Org. Process Res. Dev.* **4**:413–417 (2000).
10. A. Gavezotti. Are crystal structures predictable? *Acc. Chem. Res.* **27**:309–314 (1994).
11. J. D. Dunitz. Are crystal structures predictable? *Chem. Commun.* 545–548 (2003).
12. J. P. M. Lommerse, W. D. S. Motherwell, H. L. Ammon, J. D. Dunitz, A. Gavezotti, D. W. M. Hofmann, F. J. J. Leusen, W. T.

- M. Mooij, S. L. Price, B. Schweizer, M. U. Schmidt, B. P. van Eijck, P. Verwer, and D. E. Williams. A test of crystal structure prediction of small organic molecules. *Acta Crystallogr., B* **56**:697–714 (2000).
13. W. D. S. Motherwell, H. L. Ammon, J. D. Dunitz, A. Dzyabchenko, P. Erk, A. Gavezotti, D. W. M. Hofmann, F. J. J. Leusen, J. P. M. Lommerse, W. T. M. Mooij, S. L. Price, H. Scheraga, B. Schweizer, M. U. Schmidt, B. P. van Eijck, P. Verwer, and D. E. Williams. Crystal structure prediction of small organic molecules: a second blind test. *Acta Crystallogr., B* **58**:647–661 (2002).
 14. T. Beyer, T. Lewis, and S. L. Price. Which organic crystal structures are predictable by lattice energy minimisation? *CrystEngComm* **3**:178–212 (2001).
 15. H. Goodman and F. Gilman. *Pharmakologische Grundlagen der Arzneimitteltherapie*, McGraw-Hill, Frankfurt, p. 345, 1998.
 16. H. G. Brittain and S. R. Byrn. Structural aspects of polymorphism. *Polymorphism in Pharmaceutical Solids*. Vol. 95 Marcel Dekker, New York, 1999, pp. 73–124.
 17. D. Giron, M. Draghi, C. Goldbronn, S. Pfeffer, and P. Piechon. Study of the polymorphic behaviour of some local anaesthetic drugs. *J. Therm. Anal.* **49**:913–927 (1997).
 18. L. Kofler and A. Kofler. *Thermo-Mikro-Methoden zur Kennzeichnung organischer Stoffe und Stoffgemische*, Verlag Chemie, Weinheim, 1954.
 19. W. F. Ostwald. Studies on formation and transformation of solid materials. *Z. Phys. Chem.* **22**:289–330 (1897).
 20. A. C. Schmidt, I. Schwarz. Conformational polymorphs and pseudopolymorphs of tetracaine hydrochloride. Crystal polymorphism of local anaesthetic drugs, part IX. *J. Therm. Anal. Cal.* in press.
 21. A. C. Schmidt. Structural characteristics and crystal polymorphism of three local anaesthetic bases. Crystal polymorphism of local anaesthetic drugs, part VII. *Int. J. Pharm.* **298**:186–197 (2005).
 22. A. C. Schmidt and K. Mereiter. Polymorphism and pseudopolymorphism of salicaine and salicaine hydrochloride. Crystal polymorphism of local anaesthetic drugs, part V. *J. Pharm. Sci.*, in press.
 23. A. C. Schmidt and I. Schwarz. Solid state characterization of hydroxyprocaine. Crystal polymorphism of local anaesthetic drugs, part VIII. *J. Mol. Struct.*, **748**:153–160 (2005).
 24. V. Niederwanger. *Polymorphism Studies on Local Anaesthetics of the Amide Type*. Thesis, University of Innsbruck, Innsbruck, Austria, 2004.
 25. A. C. Schmidt, T. Brehmer, D. C. Apperley, A. King, R. K. Harris and U. J. Griesser. Three conformational polymorphs of oxybuprocaine hydrochloride. Crystal polymorphism of local anaesthetic drugs, part III, in preparation.
 26. Merck Index, 12th edn. Merck Research Laboratories, Whitehouse Station, NJ, 1996.
 27. Pharmacopeia Europaea. Europäische Arzneibuchkommission, Straßbourg, France, 2002.
 28. US Pharmacopeia XXIV. US Pharmacopeial Convention, Rockville, MD, 2000.
 29. C. Hager. *Hagers Handbuch*, Springer Verlag, Heidelberg, Germany, 1993.
 30. J. Bernstein, R. J. Davey, and J. O. Henck. Concomitant polymorphs. *Angew. Chem., Int. Ed.* **38**:3440–3461 (1999).
 31. A. C. Schmidt, N. Senfter, and U. J. Griesser. Crystal polymorphism of local anaesthetic drugs, part I: pramocaine base in comparison with pramocaine hydrochloride. *J. Therm. Anal. Calorim.* **73**:397–408 (2003).
 32. A. Burger and R. Ramberger. On the polymorphism of pharmaceuticals and other molecular crystals I. *Mikrochim. Acta* **II**:273–316 (1979).
 33. A. Burger and R. Ramberger. On the polymorphism of pharmaceuticals and other molecular crystals II. *Mikrochim. Acta* **II**:259–271 (1979).
 34. A. C. Schmidt. Solid state characterization of chlorprocaine hydrochloride. Crystal polymorphism of local anaesthetic drugs, part VI. *J. Thermal Anal. Cal.* **81**:291–297 (2005).
 35. G. A. Stephenson, E. G. Groleau, R. L. Kleemann, W. Xu, and D. R. Rigsbee. Formation of isomorphous desolvates: creating a molecular vacuum. *J. Pharm. Sci.* **87**:536–542 (1998).
 36. B. K. Sinha and V. Patabhi. Crystal structure of benzocaine—A local anesthetic. *Proc. Indian Acad. Sci., Chem. Sci.* **98**:229–234 (1987).
 37. D. E. Lynch and I. McClenaghan. Monoclinic form of ethyl 4-aminobenzoate (benzocaine). *Acta Crystallogr. E* **58**:708–709 (2002).
 38. S. Kashino, M. Ikeda, and M. Haisa. The structure of procaine. *Acta Crystallogr. B* **38**:1868–1870 (1982).
 39. R. Beall, J. Herdtklotz, and R. L. Sass. Molecular properties of local anesthetics: the crystal structure of procaine hydrochloride. *Biochem. Biophys. Res. Comm.* **39**:329–334 (1970).
 40. D. D. Dexter. Procaine: a comparative study of two independent structure determinations; conformations in different solid-state environments. *Acta Crystallogr. B* **28**:77–82 (1972).
 41. B. K. Sinha, V. Patabhi, M. Nethaji, and E. J. Gabe. Structure of a local anesthetic: dyclonine hydrochloride. *Acta Crystallogr. C* **43**:360–361 (1987).
 42. A. W. Hanson and M. Rohrl. Crystal structure of lidocaine hydrochloride monohydrate. *Acta Crystallogr. B* **28**:3567–3571 (1972).
 43. H. J. Bruins, H. J. Behm, and H. E. M. Kerckamp. Structures of the local anaesthetics ropivacaine and bupivacaine: structure determination and molecular-modelling study. *Acta Crystallogr. B* **46**:842–850 (1990).
 44. I. Csöreg. Structures and absolute configurations of enantiomers of two local anaesthetics: (2*S*)-1-Methyl- and (2*R*)-1-butyl-2',6'-piperidoxylidide hydrochlorides. *Acta Crystallogr. C* **48**:1794–1798 (1992).
 45. M. A. Bambagiotti, B. Bruni, M. Di Vaira, and V. Giannellini. (R)-(-)-Mepivacaine hydrochloride enantiomer: a low-temperature study. *Acta Crystallogr. E* **61**:585–586 (2005).
 46. A. W. Hanson and D. W. Banner. 2-Diethylamino-2',6'-acetoxylidide (lidocaine). *Acta Crystallogr. B* **30**:2486–2488 (1974).
 47. B. S. Hayward and J. Donohue. Crystal structures of two local anesthetics: dibucaine hydrochloride monohydrate and dimethisoquin hydrochloride monohydrate. *J. Cryst. Mol. Struct.* **7**:275–294 (1978).
 48. J. Donohue and B. S. Hayward. Crystal structures of two local anesthetics: dibucaine hydrochloride hydrate and dimethisoquin hydrochloride hydrate. II. Revised parameters, bond distances, and bond angles. *J. Cryst. Mol. Struct.* **10**:157–161 (1980).
 49. A. Grunenberg, J. O. Henck, and H. W. Siesler. Theoretical derivation and practical application of energy/temperature diagrams as an instrument in preformulation studies of polymorphic drug substances. *Int. J. Pharm.* **129**:147–158 (1996).
 50. A. C. Schmidt. Solid state characterisation of falicaine hydrochloride and isomorphous dyclonine hydrochloride. Crystal polymorphism of local anaesthetic drugs, part IV. *Eur. J. Pharm. Sci.* **25**:407–416 (2005).
 51. A. C. Schmidt, V. Niederwanger, and U. J. Griesser. Solid state forms of prilocaine hydrochloride. Crystal polymorphism of local anaesthetics, part II. *J. Therm. Anal. Cal.* **77**:639–652 (2004).
 52. M. Kuhnert-Brandstätter, A. Kofler, and G. Kramer. Beitrag zur mikroskopischen Charakterisierung und Identifizierung von Arzneimitteln unter Einbeziehung der UV-Spektrophotometrie. *Sci. Pharm.* **42**:150–163 (1974).
 53. J. H. Chapman, J. E. Page, A. C. Parker, D. Rogers, C. J. Sharp, and S. E. Staniforth. Polymorphism of cephaloridine. *J. Pharm. Pharmacol.* **20**:418–429 (1968).
 54. G. A. Neville and Z. R. Regnier. Hydrogen bonding in lidocaine salts. I. NH stretching band and its dependence on the associated anion. *Can. J. Chem.* **47**:4229–4235 (1969).
 55. U. Rohregger. *Phase diagrams of Terpene and Lidocaine Hydrochloride with Water*. Thesis, University of Innsbruck, Innsbruck, Austria, 1999.